
6

Terminal Osseous Dysplasia is caused by a single recurrent mutation in the FLNA Gene

Yu Sun,* Rowida Almomani,* Emmelien Aten, Jacopo Celli, Jaap van der Heijden, Hanka Venselaar, Stephen P. Robertson, Anna Baroncini, Brunella Franco, Lina Basel-Vanagaite, Emiko Horii, Ricardo Drut, Yavuz Ariyurek, Johan T. den Dunnen, Martijn H. Breuning

*These authors contributed equally to this work

Am J Hum Genet. 2010;87(1):146-53.

Summary

Terminal Osseous Dysplasia (TOD) is an X-linked dominant male-lethal disease characterized by skeletal dysplasia of the limbs, pigmentary defects of the skin and recurrent digital fibroma with onset in female infancy. After performing X-exome capture and sequencing we identified a mutation at the last nucleotide of exon 31 of the *FLNA* gene as the most likely cause of the disease. The variant c.5217G>A, was found in 6 unrelated cases (three families and three sporadic cases) and not in 400 control X chromosomes, nor pilot data from the 1000 Genomes Project or the *FLNA* gene variant database. In the families the variant segregated with the disease and it was transmitted four times from a mildly affected mother to a more seriously affected daughter. We show that, due to non-random X-inactivation, the mutant allele was not expressed in patient fibroblasts. RNA expression of the mutant allele was only detected in cultured fibroma cells obtained from 15-year old surgically removed material. The variant activates a cryptic splice site, removing the last 48 nucleotides from exon 31. At the protein level this results in a loss of 16 amino acids (p.Val1724_Thr1739del), predicted to remove a sequence at the surface of filamin repeat 15. Our data show that TOD is caused by this single recurrent mutation in the *FLNA* gene.

Terminal Osseous Dysplasia (OMIM 300244) is a rare condition, characterized by terminal skeletal dysplasia, pigmentary defects of the skin, and recurrent digital fibromata during infancy. It has been described as a male-lethal X-linked dominant disease in the previously reported families and cases[1]. Linkage studies mapped the mutation to Xq27.3-q28[2]. However, no disease-causing gene was discovered yet.

In the present study, we examined TOD in three families and three sporadic cases (patients 1, 2 and 3 described by Horii[3], Drut[4] and Breuning[5]). The Dutch (Figure 1A, family 1) and Italian families (Figure 1A, family 2) have been described before (Breuning[5] and Baroncini[6]). The third family (Figure 1A, family 3) has not been reported before, it is non-consanguineous and of Israeli-Arab origin. All patients, a mother and her two daughters have normal cognitive development. The mother (3I:2) suffers from chronic mild obstructive lung disease and vitamin B12 deficiency. Since her childhood she had multiple minor surgeries to remove small skin lesions from her hands and legs. On clinical examination at age 25 years her head circumference was 54 cm (25-50%), height 170 cm (75-90%), arm span 171 cm. Her right hand showed brachydactyly of digit III-V, a short fingernail on digitus IV and lateral deviation of the 5th digit. On her left hand there was lateral deviation of the 4th digit with a small lesion on the lateral aspect of the distal phalanx and clinodactyly of the 5th digit (Figure 1B). Her right foot showed a short and highly implanted 4th digit. There was bilateral widening of the distal portion of the 2nd-5th digit. She had no gingival extra frenulum and no pterygium. A skeletal X-ray survey revealed unilateral flattening of her vertebral bodies at L1-L3, secondary right scoliosis and wedging of her L1 vertebral body. Her daughter (3II:4) underwent surgery at 2 months of age to remove small skin lesions from her hands, feet and gingiva. On clinical examination at age three she had a head circumference of 48 cm (25-50%), a height of 85 cm (<3%) and a of weight 11.1 kg (<3%). She showed hypertelorism - interpupillary distance of 5.4cm (>97%), a right epicanthal fold, a normal palate, an upper and lower accessory frenulum (Figure 1C), a short neck and a short thorax. Despite earlier surgery, she had bilateral skin lesions on her 2nd and 5th digits and bilateral clinodactyly of the 5th digit (Figure 1D). Her feet showed a lesion in her 3rd toes and thickening of the nail of the 5th toes bilaterally. A skeletal X-ray survey revealed bilateral lytic lesions in the proximal humerus, the proximal femur, and multiple soft tissue lesions in her feet and hands. The youngest daughter (3II:5) was born with multiple lesions on her hands and feet including bilateral camptodactyly of the 3rd digit, and bilateral overriding of the 4th toe. On the echocardiogram she had persistent foramen ovale at birth. On clinical examination at age six months her head circumference was 42 cm (25-50%), height 58.8 cm (<3%) and weight 5.1 kg (<3%). She has mild hypertelorism, three brownish pigmented spots of different size (3 mm to 1.5 cm) in her right temporal groove, mild retrognathia, a right upper accessory frenulum and a cleft palate, a short neck and a

short thorax. She has a bilateral axillary pterygium (Figure 1E), which is more severe on the right side. Bilaterally, there is limited extension of her elbows with normal supination and pronation of her hands. In her right hand (Figure 1F) she had multiple skin lesions on her 2nd - 5th digits, clinodactyly and lateral deviation of her 2nd and 3rd digits and a narrow 5th digit with an absent distal crease. Her left hand showed skin lesions on her 2nd - 4th digits. Her 2nd digit was narrow and laterally deviated. There was camptodactyly of the 3rd-5th digits, brachydactyly and clinodactyly of the 5th digit and absence of a distal crease. In her feet she had bilateral plantar pits. The right foot has distal broadening of 2nd-5th toe, brachydactyly of the 2nd and 3rd toe accompanied by syndactyly. There was overriding of the 3rd and 4th toe. On her left foot the 2nd-5th toes were distally broad. She had a overlapping of the 2nd and 4th toes over her 3rd toe, brachydactyly of the 3rd

Figure 1: The pedigrees and the phenotype of family 3. (A) The pedigrees investigated in this study, in family 3 X inactivation patterns show the silencing of the X chromosome which carries the mutant allele. (B) shows the hands of 3I:2. (C) Multiple frenula of 3II:4. (D) The right hands of 3II:4. She has clinodactyly and digital fibroma. (E) shows the right upper accessory frenulum of 3II:5. (F) The right hand of 3II:5.

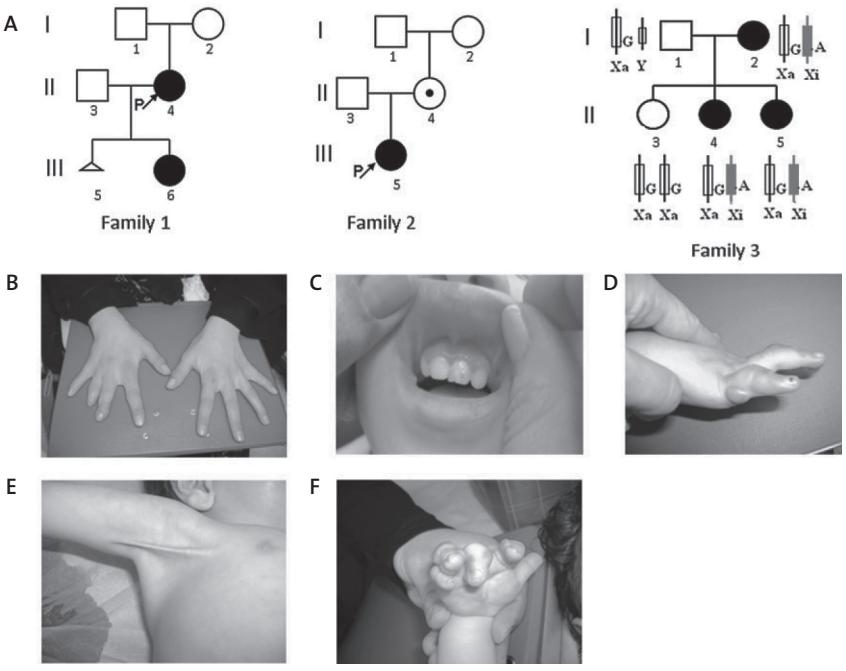

toe that was a high implanted. A skeletal X-ray survey revealed bilateral lytic lesions of the proximal humerus, lytic lesions of the left proximal femur, and multiple soft tissue lesions. She had underdeveloped tarsal bones in her feet. The phenotypes from different patients are summarized in Table 1.

DNA of patients and family members were extracted from peripheral blood (family 1, 2, 3), buccal cells (patient 1) or paraffin embedded tissue (patient 2, 3). Two probands (1II:4, 2III:5) of the Dutch and the Italian families were tested using the X-exome target enrichment methodology (SureSelect, Agilent) and next generation sequencing (Illumina Genome Analyzer II). The methods used for sequence capture, enrichment and elution followed instructions and protocols provided by the manufacturers (SureSelect, Agilent) with a little modification. In brief, 500ng of DNA was fragmented (Bioruptor, Diagenode) according to manufacturer's instructions to yield fragments from 200-300 bp. Paired-end adaptor oligonucleotides from Illumina were added to both ends. The DNA-adaptor ligated fragments were then hybridized to 250ng of SureSelect X-chromosome Oligo capture library (SureSelect, Agilent) for 14 hours. After Hybridization, washing and elution, the elute was amplified to create sufficient DNA template for downstream applications. The eluted-enriched DNA fragments were sequenced using the Illumina technology platform. We prepared the paired–end flow-cell on the supplied cluster station following the instructions of the manufacturer.

The reads were aligned to the reference human genome (hg 18, NCBI Build 36.2) by Bowtie[7] (Supplementary Table S1). Substitution variant calling was performed by searching for positions where a variant nucleotide was present in more than 30% of the reads. After removing substitutions present with high frequency in dbSNP, the variants located in the previously identified TOD linkage interval, Xq27.3-q28, were listed in Table 2. From these variants, c.5217G>A, the only variant shared by the two patients, in the *FLNA* gene were selected for further study because; (i) c.5217G>A, the last nucleotide of exon 31, was predicted to affect splicing by Human Splicing Finder[8]. The score of splicing donor site dropped from 91.2 to 80.63, indicating the wild type site may not function as usual, (ii) mutations in *FLNA* have been reported to be involved in diseases showing a partial phenotypic overlap with TOD[9].

Sanger sequencing results confirmed the presence of c.5217G>A (Figure 2A) and c.5850T>C (Figure 2B) in all affected cases (1II:4, 1III:6) in family 1 as well as c.5686+84A>G found in an intron, but not in an unaffected individual (1I:2). Further evidence came from the analysis of the Italian family where affected cases (2II:4, 2III:5) carry exactly the same variant; c.5217G>A, here together with another exonic variant c.5814C>T. Unfortunately, we did not have access to material from both parents and therefore we could not determine whether the mutations occurred de novo.

Table 1. Clinical features of the patients studied in this report.

	1II:4	1III:6	2II:4	2III:5	3I:2	3II:4	3 II:5	Patient 1	Patient 2	Patient 3
Origin	Dutch	Dutch	Italian	Italian	Israeli-Arab	Israeli-Arab	Israeli-Arab	Japanese	Argentina	Dutch
Age of onset	1 mo	3 mo		7 mo		2 mo	birth	3 mo		4 mo
Pigmentary skin anomalies										
Face	+	+	-	+			+	+	+	+
Scalp	-							-	+	-
Fibromatosis										
Digital fibromas	+	+	-	+	+	+	+	+	+	+
Limbs and skeletal system										
Synadactyly	-	-	-	+		+	+	-	-	-
Brachydactyly	+		-	+	+		+	+		
Clinodactyly			-	+	+	+	+			
Camptodactyly				+			+			
Metacarpal disorganization	+	+	-	+				+	+	+
Metatarsal disorganization	+	+	-	+			+	+	+	+
Limb long bones anomalies	-	+	-	+	-	+	+	+	+	+
Articular abnormalities	+	+	-	+				+	+	+
Facial and mouth Features										
Cleft palate	-	-	-	-		-	+	-	-	
Upslanting palpebral fissures	-		-	+				+		
Hypertelorism/Telecanthus	+		-	-		+	+	+		
Epicanthic folds	-		-	+		+		+		
Coloboma of Iris	-	+	-	-				-	-	-
Flat/depressed nasal tip	-	+	-	-				+	-	
Thick lips/Prominent	+		-	+						
Lower lip										
Papillomata	-	-	-							-
Multiple frenula			+	+	-					
Preauricular pits and tags	+							-		

Table 2: List of all exonic variants with low frequency in the European population in Xq27.3-Xq28.

HGVS name	Gene	Predicted Function	Predicted Protein Change	1II:4	2III:5	
NM_002025.2:c.1653A>G	*AFF2*	Silent	p.(=)	-	+	
NM_001183.4:c.*461A>C	*ATP6AP1*	3' UTR	p.(=)	-	+	
NM_001009932.1:c.364G>A	*DNASE1L1*	Silent	p.(=)	+	-	
NM_001110556.1:c.5217G>A	*FLNA*	Silent	p.(=)	+	+	
NM_001110556.1:c.5814C>T	*FLNA*	Silent	p.(=)	-	+	rs2070825, high frequency in a group of multiple population
NM_001110556.1:c.5850T>C	*FLNA*	Silent	p.(=)	+	-	Doesn't segragate with phenotype
NM_004961.3:c.186G>A	*GABRE*	Silent	p.(=)	+	-	
NM_005342.2:c.166G>C	*HMGB3*	Missense	p.(Glu56Gln)	-	+	
NM_005367.4:c.888A>G	*MAGEA12*	Silent	p.(=)	-	+	
NM_005362.3:c.455G>T	*MAGEA6*	Missense	p.(Ser152Ile)	+	-	Repetitive region
NM_005365.4:c.92C>A	*MAGEA9*	missense	p.(Pro31His)	+	-	Repetitive region
NM_001170944.1:c.468C>T	*PNMA6B*	Silent	p.(=)	+	-	
NM_005629.3:c.324A>G	*SLC6A8*	Silent	p.(=)	-	+	
NM_032539.2:c.1002T>C	*SLITRK2*	Silent	p.(=)	-	+	
NM_032539.2:c.309G>A	*SLITRK2*	Silent	p.(=)	-	+	
NM_001009615.1:c.240C>A	*SPANXN2*	Silent	p.(=)	+	-	
NM_014370.2:c.1014G>A	*SRPK3*	Silent	p.(=)	+	-	
NM_006280.1:c.430G>A	*SSR4*	Missense	p.(Gly144Arg)	+	-	

All of the HGVS numbers were generated with the use of the longest isoforms if multiple transcripts existed.

Notably, families 1 and 2 had two distinct variants adjacent to the c.5217G>A mutation, making a close and common ancestor highly unlikely. Finally, upon analysis of a third TOD family and three unrelated sporadic cases, we identified exactly the same c.5217G>A variant again in all patients, but not unaffected family members (1I:2, 3I:1 and 3II:3).

Variant c.5217G>A affects the last nucleotide of exon 31 of the *FLNA* gene (Figure 2C). At protein level, it is not predicted to change the encoded amino acid but as the last nucleotide of an exon, it may affect splicing[10-12]. RNA was isolated from cultured fibroblasts of arm skin from 1III:6, removed during a recent orthopaedic procedure under general anaesthesia with informed consent. Cells were cultured in standard medium for human fibroblasts (DMEM with 10%FBS, 1%Pen/Strep, 1%glucose, 1%glutamax) with 5%CO_2 in 37°C. RNA was extracted by RNeasy Mini Kit (QIAGEN). cDNA was synthesized from 500ng of total RNA by RevertAid RNaseH- M-MuLV reverse transcriptase in a total volume of 20 µL according to the protocol provided by the supplier (MBI-Fermentas). Target regions were amplified by RT-PCR using the primers listed in Supplementary data S2. The products were evaluated using Bioanalyzer 2100 DNA chip 1000 (Agilent) according to the manufacturers instruction. RNA from patient fibroblasts showed only normal transcripts, both of transcripts 1 (NM_01456) and 2 (NM_001110556), differing by insertion of the 24 bp exon 30 in transcript 2. Although transcript 1 has been reported as the predominant transcript in controls[13], we detected about equal expression levels in controls (Figure 3B lane 2-4, 8) and higher expression of transcript 2 in patient fibroblasts (Figure 3B lane 1). Both bands were isolated from the agarose gel by Qiaquick gel extraction kit (QIAGEN) and analysed by Sanger sequencing. Interestingly, we detected no expression of the mutant allele. This could be due to nonsense mediated decay (NMD)[14] and/or skewed X chromosome inactivation (XCI). To test the first possibility, the fibroblasts were treated with cycloheximide[15] for 4.5 hours followed by RNA analysis using the same procedures as for RNA from untreated cells. The mutant allele was still absent in RNA from cycloheximide treated cells. X-inactivation was analysed using the Androgen Receptor (AR) Assay[16]. The assay showed random X-inactivation in 1I:2 versus 100% X-inactivation of the mutant chromosome in patient 1II:4 (patient 1III:6 was uninformative), indicating that the mutant allele was inactivated.

Fifteen years ago, at the age of 1 year, fibroma tissue was surgically removed and stored in liquid nitrogen from the 5th digits of both hands and the 5th toe of the left foot of patient 1III:6. We cultured these cells, and analysed RNA. In the fibroma cells we observed 2 sets of 2 bands (Figure 3B lane 5-7), indicating altered splicing. One set had the same length as observed in normal fibroblasts (Figure 3A transcript 1 and 2), the other set was shorter (Figure 3A transcript 3 and 4, faint from RNA of tumor in left fifth finger and toe, Figure 3B lane 6 and 7 respectively). Note that the fibroma always contains a mixture of tumor and normal stroma cells.

Figure 2: Genomic Structure and mutation analysis of *FLNA*. (A) c.5217G>A was confirmed by Sanger sequencing in all the patients. The unaffected family members and controls carry the homozygous normal allele. (B) shows the sequence of c.5850T>C in family 1. (C) FLNA is located in Xq28, the target region of linkage analysis. C.5217G>A alters the last nucleotide of exon 31 of FLNA.

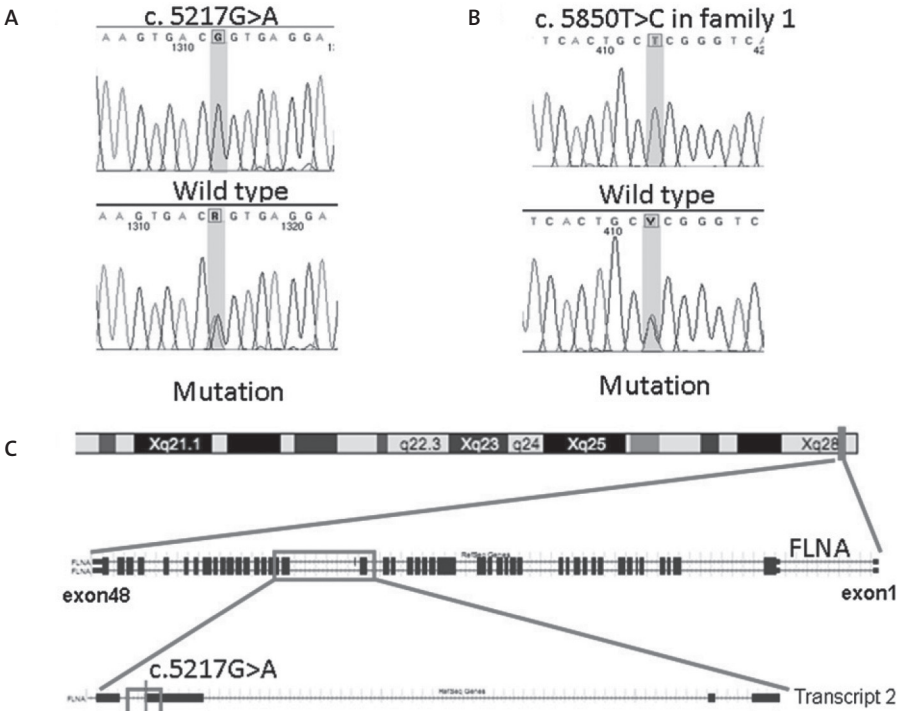

Sequence analysis showed a deletion removing the last 48 nucleotides of exon 31 (Figure 3C), resulting in a deletion of 16 amino acids.

To facilitate clinical diagnostics of *FLNA* gene mutations we have established a web-based *FLNA* gene variant database using the LOVD software[17]. In this publicly available database we have collected all variants reported in literature thus far (83 in total, see *FLNA* mutation database), incl. the new variants described here. The c.5217G>A variant detected in TOD patients has not been described before; it is neither listed in dbSNP nor in the pilot study 1 of the 1000 Genomes Project. Finally, >400 chromosomes have been sequenced and the mutant allele was not found (data not shown).

Mutations in *FLNA* have been reported to cause a wide range of developmental malformations in brain, bone, limbs, heart[18] and other organs[19] in human[9], including periventricular heterotopia (PVNH) (OMIM 300049)[20-24] and OPD spectrum disorders[25] which include otopalatodigital syndrome type 1 (OMIM 311300)[26-28] and 2 (OMIM 304120)[26; 29], frontometaphyseal dysplasia (OMIM 305620) [26; 30-31] and Melnick-Needles syndrome (OMIM 309350)[26-27]. Although each of OPD spectrum disorders are characterized by specific clinical symptoms, there clearly is a clinical overlap with TOD including a generalized bone dysplasia including craniofacial anomalies, digits and long bones[9; 32]. Interestingly, the most conspicuous symptoms of TOD patients are skeletal dysplasia of the limbs and recurrent digital fibroma, suggesting a significant role of the *FLNA* mutation in the TOD phenotype.

The *FLNA* gene encodes a cytoskeletal protein, filamin A, which crosslinks actin filaments into an orthogonal network and links these to the cell membrane. Within the cytoskeleton filamin A also mediates functions relating to cell signaling, transcription and development[33]. Filamin A consists of two calponin homology sequences (CH1 and CH2) at the N-terminal and connects with 24 immunoglobin like filamin repeats, divided by 2 hinges between repeat 15 and 16, repeat 23 and 24. To check the stability of filamin A in patient cells, protein was extracted from both fibroblast and fibroma cells. Western blot was performed using mouse anti-human filamin A monoclonal antibody, MAB1680, from MILLIPORE. No difference was observed on molecular weight or quantity. Likely the difference of 18 amino acids was too small to distinguish by western blot. The c.5217G>A mutation is located in a highly conserved position at the DNA level across a wide range of vertebrate and invertebrate species except rodent, found in all ten affected patients from six different unrelated families. In addition, the mutation introduced abnormal splicing in fibroma cells. At protein level, c.5217G>A encodes the second last amino acid of repeat 15, which is immediately adjacent to hinge 1. Recent studies demonstrated repeat 9-15 contain an F-actin binding domain necessary for high avidity F-actin binding[34]. Hinge 1 plays an important part in maintaining the viscoelastic properties of actin networks[35]. Moreover, this region interacts with many binding partners like TRAF1, TRAF2[36], CaR extracellular Ca^{2+} receptor[37], and FAP52[38]. As no crystal structure has yet been described for this region, the crystal structure of repeat 15 in filamin B(PDB file 2dmb), that shows the highest identity (58%) with this region of interest, was used as a template to build a 3D model (Figure 3D). The model was built using the WHAT IF &Yasara twinset[39]. Repeat 15 consists of 2 beta-sheets. The in-frame deletion causes the removal of the top of a beta-strand in the middle of one beta-sheet, and of two beta-strands at the side of that sheet (grey part of Figure 3D). These residues are likely to form some kind of beta-strand like structure, and substantially alter the structure of the highly conserved tertiary structure of filamin

repeat 15. Furthermore, this structure will affect the residues following the beta-sheet and linking repeat 15 to hinge1. Although there is no way to predict what will happen to those linking residues, we believe it will affect the overall conformation of the protein, and likely influence the interaction between filamin A and other molecules.

Figure 3: Detection of alternative splicing and 3D protein model. (A) Diagram of four FLNA transcripts in fibroma cells: transcript 1 and 2, which carry the 48bp deletion at the end of exon 31, as well as the normal transcripts 3 and 4. (B) RT-PCR result from Agilent 2100 Bioanalyzer. Lane 1 is the product of the fibroblasts of 1III:6, which has a predominant longer isoform. Lane 2-4 and 8 are four control human fibroblasts. Lanes 5-7 show RT-PCR products that were obtained from fibroma cells of 1III:6, the normal bands from two FLNA isoforms, and two extra shorter bands, which are faint in lane 6 (left fifth finger)and lane 7 (fifth toe of the left foot) , whereas lane 5 (right fifth finger)shows four dark bands. (C) Sanger sequencing results of c.5858T>C and c.5217G>A in fibroblast and fibroma cells of 1III:6. (D) The 3D model of FLNA domain 15. The deleted 16 amino acids are marked in gray. Beta-strands are marked in red. Green represents a turn. Yellow indicates a 3/10 helix. Random coils are colored in cyan.

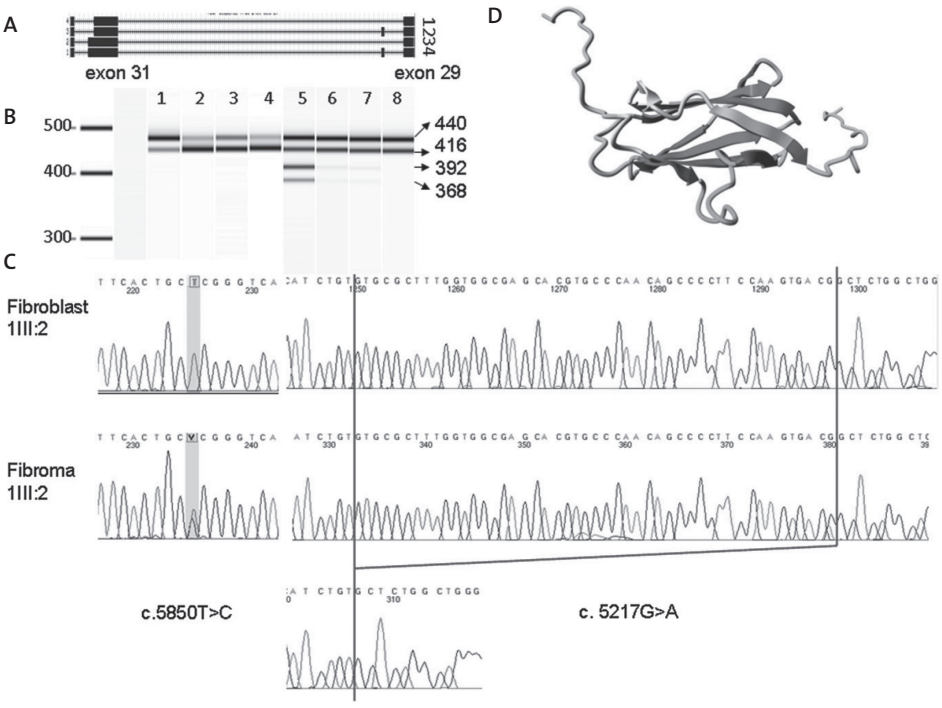

The precise mechanism of TOD remains unclear. However, like other X-linked diseases, X chromosome inactivation (XCI) might be a key component of how the disease develops. The developmental role of *FLNA* is borne out by the presence of the skeletal and skin malformations at birth. Multiple fibroma on digits start occurring in the first years. Fibromas spontaneously stop by the age of five. Skewed XCI is known to vary in different tissues and to correlate with age under the pressure of secondary selection[40]. Several mechanisms may contribute to the skewing, including stochastic effects, a selective growth advantage of cell that carries either the mutated or the normal allele (secondary cell selection) and genetic processes yielding preferential inactivation of specific alleles. Primarily the X inactivation choice is random, but during cell proliferation either in all cells or in a tissue specific manner, cells that carry an activate mutated allele may have a significant disadvantage, are gradually lost or selected against and are thus less represented in the adult female[41]. Disorders caused by defects in *FLNA* gene often show skewed XCI pattern[26], suggesting that cells need normal filamin to survive. Several studies in TOD families, showed patients had skewed X-inactivation, while unaffected individuals had random inactivation[1, 6]. We examined the X-inactivation pattern in family 1 (1I:2, 1II:4 and 1III:6) and 3 (3I:2, 3II:3, 3II:4 and 3II:5, Figure 1A) by AR assay. Apart from the uninformative 1III:6, all the patients, 1II:4, 3I:2, 3II:4 and 3II:5 showed extremely skewed X-inactivation (0/100%), while the normal family member 1I:2 showed random X-inactivation (30/70%) together with 3II:3 (50/50%). Since there was no mutant allele detectable in the RNA of normal fibroblast, we deduced 1III:6 also had 100% skewed XCI with the preferential inactivation of the mutant allele. Baroncini tested the XCI of 2II:4 and 2III:5, and both showed 100% skewing[6]. 2II:4 was interpreted by the authors as unaffected. However, we assume 2II:4 is a carrier of TOD, as she only has mild manifestations (multiple frenula in the mouth). She probably has skewed X-inactivation at a very early stage. Overall as well as local X inactivation patterns may influence the severity of the phenotype of carrier females and are also associated with selective female survival in male lethal X-linked dominant disorders.

Taken together, these data suggest that TOD unique variant c.5217G>A (p.Val1724_Thr1739del) in the *FLNA* gene. The variant is not found in other databases, has not been seen in other patients with pathogenic *FLNA* variants, segregates with the disease, and locates in Xq28 where the potential mutated gene causing this disorder was mapped previously. The mutation was found in six unrelated families. It will affect splicing, and causes a deletion of 16 amino acids in protein level. The missing region in the filamin A protein is hypothesized to affect or prevent the interaction of filamin A with other proteins.

Acknowledgements

We would like to thank the patients and their family members for their willingness to join the project, CSC scholarship for supporting Yu Sun's studies in the Netherlands, Filip Kluin for sending and Hans Morreau for isolating DNA from paraffin embedded tissue, Tobias Messemaker for helping us with western blot, the Leiden Genome Technology Center (LGTC), and Laboratory for Diagnostic Genome Analysis (LDGA) for help with sequencing, DNA extraction, X-inactivation detection. X-exome capture was implemented in collaboration with ServiceXS (Leiden, www.servicexs.com). The research leading to these results has received funding from the European Community's Seventh Framework Program (FP7/2007-2013) under grant agreements 223026 (NMD-chip), 223143 (TechGene) and 200754 (Gen2Phen).

Web Resource

Accession numbers and URLs for data presented herein are as follows:
FLNA gene variant database, http://www.lovd.nl/FLNA
SureSelect manual, http://www.genomics.agilent.com/files/Manual/G3360-90020_SureSelect_Indexing_1.0.pdf
UCSC Genome Browser, http://genome.ucsc.edu/
Online Mendelian Inheritance in Man(OMIM), http://www.ncbi.nlm.nih.gov/entrez/Omim/
RefSeq, http://www.ncbi.nlm.nih.gov/Refseq/, for human FLNA[accession number NM_001110556.1], for human chromosome X [accesssion number NC_000023.9]
dbSNP, http://www.ncbi.nlm.nih.gov/projects/SNP/
1000 genome project, http://www.1000genomes.org/page.php
Bowtie, http://bowtie-bio.sourceforge.net/index.shtml
Human Splicing Finder, http://www.umd.be/HSF
YASARA, http://www.yasara.org/

1. Bacino, C.A., Stockton, D.W., Sierra, R.A., Heilstedt, H.A., Lewandowski, R., and Van den Veyver, I.B. (2000). Terminal osseous dysplasia and pigmentary defects: clinical characterization of a novel male lethal X-linked syndrome. Am J Med Genet 94, 102-112.

2. Zhang, W., Amir, R., Stockton, D.W., Van Den Veyver, I.B., Bacino, C.A., and Zoghbi, H.Y. (2000). Terminal osseous dysplasia with pigmentary defects maps to human chromosome Xq27.3-xqter. Am J Hum Genet 66, 1461-1464.

3. Horii, E., Sugiura, Y., and Nakamura, R. (1998). A syndrome of digital fibromas, facial pigmentary dysplasia, and metacarpal and metatarsal disorganization. Am J Med Genet 80, 1-5.

4. Drut, R., Pedemonte, L., and Rositto, A. (2005). Noninclusion-body infantile digital fibromatosis: a lesion heralding terminal osseous dysplasia and pigmentary defects syndrome. Int J Surg Pathol 13, 181-184.

5. Breuning, M.H., Oranje, A.P., Langemeijer, R.A., Hovius, S.E., Diepstraten, A.F., den Hollander, J.C., Baumgartner, N., Dwek, J.R., Sommer, A., and Toriello, H. (2000). Recurrent digital fibroma, focal dermal hypoplasia, and limb malformations. Am J Med Genet 94, 91-101.

6. Baroncini, A., Castelluccio, P., Morleo, M., Soli, F., and Franco, B. (2007). Terminal osseous dysplasia with pigmentary defects: clinical description of a new family. Am J Med Genet A 143, 51-57.

7. Langmead, B., Trapnell, C., Pop, M., and Salzberg, S.L. (2009). Ultrafast and memory-efficient alignment of short DNA sequences to the human genome. Genome Biol 10, R25.

8. Desmet, F.O., Hamroun, D., Lalande, M., Collod-Beroud, G., Claustres, M., and Beroud, C. (2009). Human Splicing Finder: an online bioinformatics tool to predict splicing signals. Nucleic Acids Res 37, e67.

9. Robertson, S.P. (2005). Filamin A: phenotypic diversity. Curr Opin Genet Dev 15, 301-307.

10. Agarwal, N., Kutlar, F., Mojica-Henshaw, M.P., Ou, C.N., Gaikwad, A., Reading, N.S., Bailey, L., Kutlar, A., and Prchal, J.T. (2007). Missense mutation of the last nucleotide of exon 1 (G->C) of beta globin gene not only leads to undetectable mutant peptide and transcript but also interferes with the expression of wild allele. Haematologica 92, 1715-1716.

11. Yamada, K., Fukao, T., Zhang, G., Sakurai, S., Ruiter, J.P., Wanders, R.J., and Kondo, N. (2007). Single-base substitution at the last nucleotide of exon 6 (c.671G>A), resulting in the skipping of exon 6, and exons 6 and 7 in human succinyl-CoA:3-ketoacid CoA transferase (SCOT) gene. Mol Genet Metab 90, 291-297.

12. Kuivaniemi, H., Tromp, G., Bergfeld, W.F., Kay, M., and Helm, T.N. (1995). Ehlers-Danlos syndrome type IV: a single base substitution of the last nucleotide of exon 34 in COL3A1 leads to exon skipping. J Invest Dermatol 105, 352-356.

13. Maestrini, E., Patrosso, C., Mancini, M., Rivella, S., Rocchi, M., Repetto, M., Villa, A., Frattini, A., Zoppe, M., Vezzoni, P., et al. (1993). Mapping of two genes encoding isoforms of the actin binding protein ABP-280, a dystrophin like protein, to Xq28 and to chromosome 7. Hum Mol Genet 2, 761-766.

14. Holbrook, J.A., Neu-Yilik, G., Hentze, M.W., and Kulozik, A.E. (2004). Nonsense-mediated decay approaches the clinic. Nat Genet 36, 801-808.

15. Kim, C.E., Gallagher, P.M., Guttormsen, A.B., Refsum, H., Ueland, P.M., Ose, L., Folling, I., Whitehead, A.S., Tsai, M.Y., and Kruger, W.D. (1997). Functional modeling of vitamin responsiveness in yeast: a common pyridoxine-responsive cystathionine beta-synthase mutation in homocystinuria. Hum Mol Genet 6, 2213-2221.

16. Kubota, T., Nonoyama, S., Tonoki, H., Masuno, M., Imaizumi, K., Kojima, M., Wakui, K., Shimadzu, M., and Fukushima, Y. (1999). A new assay for the analysis of X-chromosome inactivation based on methylation-specific PCR. Hum Genet 104, 49-55.

17. Fokkema, I.F., den Dunnen, J.T., and Taschner, P.E. (2005). LOVD: easy creation of a locus-specific sequence variation database using an "LSDB-in-a-box" approach. Hum Mutat 26, 63-68.

18. Kyndt, F., Gueffet, J.P., Probst, V., Jaafar, P., Legendre, A., Le Bouffant, F., Toquet, C., Roy, E., McGregor, L., Lynch, S.A., et al. (2007). Mutations in the gene encoding filamin A as a cause for familial cardiac valvular dystrophy. Circulation 115, 40-49.

19. Gargiulo, A., Auricchio, R., Barone, M.V., Cotugno, G., Reardon, W., Milla, P.J., Ballabio, A., Ciccodicola, A., and Auricchio, A. (2007). Filamin A is mutated in X-linked chronic idiopathic intestinal pseudo-obstruction with central nervous system involvement. Am J Hum Genet 80, 751-758.

20. Fox, J.W., Lamperti, E.D., Eksioglu, Y.Z., Hong, S.E., Feng, Y., Graham, D.A., Scheffer, I.E., Dobyns, W.B., Hirsch, B.A., Radtke, R.A., et al. (1998). Mutations in filamin 1 prevent migration of cerebral cortical neurons in human periventricular heterotopia. Neuron 21, 1315-1325.

21. Sheen, V.L., Dixon, P.H., Fox, J.W., Hong, S.E., Kinton, L., Sisodiya, S.M., Duncan, J.S., Dubeau, F., Scheffer, I.E., Schachter, S.C., et al. (2001). Mutations in the X-linked filamin 1 gene cause periventricular nodular heterotopia in males as well as in females. Hum Mol Genet 10, 1775-1783.

22. Moro, F., Carrozzo, R., Veggiotti, P., Tortorella, G., Toniolo, D., Volzone, A., and Guerrini, R. (2002). Familial periventricular heterotopia: missense and distal truncating mutations of the FLN1 gene. Neurology 58, 916-921.

23. Zenker, M., Rauch, A., Winterpacht, A., Tagariello, A., Kraus, C., Rupprecht, T., Sticht, H., and Reis, A. (2004). A dual phenotype of periventricular nodular heterotopia and frontometaphyseal dysplasia in one patient caused by a single FLNA mutation leading to two functionally different aberrant transcripts. Am J Hum Genet 74, 731-737.

24. Sheen, V.L., Jansen, A., Chen, M.H., Parrini, E., Morgan, T., Ravenscroft, R., Ganesh, V., Underwood, T., Wiley, J., Leventer, R., et al. (2005). Filamin A mutations cause periventricular heterotopia with Ehlers-Danlos syndrome. Neurology 64, 254-262.

25. Robertson, S.P. (2007). Otopalatodigital syndrome spectrum disorders: otopalatodigital syndrome types 1 and 2, frontometaphyseal dysplasia and Melnick-Needles syndrome. Eur J Hum Genet 15, 3-9.

26. Robertson, S.P., Twigg, S.R., Sutherland-Smith, A.J., Biancalana, V., Gorlin, R.J., Horn, D., Kenwrick, S.J., Kim, C.A., Morava, E., Newbury-Ecob, R., et al. (2003). Localized mutations in the gene encoding the cytoskeletal protein filamin A cause diverse malformations in humans. Nat Genet 33, 487-491.

27. Robertson, S.P., Thompson, S., Morgan, T., Holder-Espinasse, M., Martinot-Duquenoy, V., Wilkie, A.O., and Manouvrier-Hanu, S. (2006). Postzygotic mutation and germline mosaicism in the otopalatodigital syndrome spectrum disorders. Eur J Hum Genet 14, 549-554.

28. Hidalgo-Bravo, A., Pompa-Mera, E.N., Kofman-Alfaro, S., Gonzalez-Bonilla, C.R., and Zenteno, J.C. (2005). A novel filamin A D203Y mutation in a female patient with otopalatodigital type 1 syndrome and extremely skewed X chromosome inactivation. Am J Med Genet A 136, 190-193.

29. Marino-Enriquez, A., Lapunzina, P., Robertson, S.P., and Rodriguez, J.I. (2007). Otopalatodigital syndrome type 2 in two siblings with a novel filamin A 629G>T mutation: clinical, pathological, and molecular findings. Am J Med Genet A 143A, 1120-1125.

30. Zenker, M., Nahrlich, L., Sticht, H., Reis, A., and Horn, D. (2006). Genotype-epigenotype-phenotype correlations in females with frontometaphyseal dysplasia. Am J Med Genet A 140, 1069-1073.

31. Giuliano, F., Collignon, P., Paquis-Flucklinger, V., Bardot, J., and Philip, N. (2005). A new three-generational family with frontometaphyseal dysplasia, male-to-female transmission, and a previously reported FLNA mutation. Am J Med Genet A 132A, 222.

32. Robertson, S.P. (2004). Molecular pathology of filamin A: diverse phenotypes, many functions. Clin Dysmorphol 13, 123-131.

33. Zhou, A.X., Hartwig, J.H., and Akyurek, L.M. (2010). Filamins in cell signaling, transcription and organ development. Trends Cell Biol 20, 113-123.

34. Nakamura, F., Osborn, T.M., Hartemink, C.A., Hartwig, J.H., and Stossel, T.P. (2007). Structural basis of filamin A functions. J Cell Biol 179, 1011-1025.

35. Gardel, M.L., Nakamura, F., Hartwig, J.H., Crocker, J.C., Stossel, T.P., and Weitz, D.A. (2006). Prestressed F-actin networks cross-linked by hinged filamins replicate mechanical properties of cells. Proc Natl Acad Sci U S A 103, 1762-1767.

36. Arron, J.R., Pewzner-Jung, Y., Walsh, M.C., Kobayashi, T., and Choi, Y. (2002). Regulation of the subcellular localization of tumor necrosis factor receptor-associated factor (TRAF)2 by TRAF1 reveals mechanisms of TRAF2 signaling. J Exp Med 196, 923-934.

37. Awata, H., Huang, C., Handlogten, M.E., and Miller, R.T. (2001). Interaction of the calcium-sensing receptor and filamin, a potential scaffolding protein. J Biol Chem 276, 34871-34879.

38. Nikki, M., Merilainen, J., and Lehto, V.P. (2002). FAP52 regulates actin organization via binding to filamin. J Biol Chem 277, 11432-11440.

39. Krieger, E., Koraimann, G., and Vriend, G. (2002). Increasing the precision of comparative models with YASARA NOVA--a self-parameterizing force field. Proteins 47, 393-402.

40. Sharp, A., Robinson, D., and Jacobs, P. (2000). Age- and tissue-specific variation of X chromosome inactivation ratios in normal women. Hum Genet 107, 343-349.

41. Orstavik, K.H. (2009). X chromosome inactivation in clinical practice. Hum Genet 126, 363-373.

Supplementary information

Table S1: The overview of the data generated by GAII.

	1II:4	2III:5
Run	Paired-end	Paired-end
Total reads	36,010,190	28,960,586
Read F	18,005,095	14,480,293
Read R	18,005,095	14,480,293
Aligned reads	33,054,043	18.948,705
Aligned in pair	30,018,244	11,012,526
Read length	51	51

Table S2: F LNA primer list.

location		Primer sequences (5'-3')	Size (bp)
Exon 31-32	DNA (blood, buccal cells)	F:GTCATCTGTGTGCGCTTTGG	222
		R:AGCTGCTGAGACCGTAGAGG	
Exon 31	DNA (paraffin embedded tissue)	F:GGGCAAATACGTCATCTGTGT	104
		R:agacacccctgctgacctac	
Exon 29-32	RNA	F:CCTGGGCGTAGGTGTACTGT	416 (short isoform)
		R:CATCAAGTACGGTGGTGACG	440 (long isoform)
Exon 35-37	DNA, RNA	F:ACATACGCATGGAGTCGTCA	577 (DNA)
		R:TCAACTGTGGCCATGTCACT	294 (RNA)

Figure S3: The 2100 bioanalyzer traces of RT-PCR on c.5217G>A from lane 1 to 8. The peak around 15 bp is the lower ladder and the signal round 1500 bp is the upper ladder.